

# Applications of satellite remote sensing to the marine environment in Western Australia

A Pearce<sup>1</sup> & C Pattiaratchi<sup>2</sup>

<sup>1</sup> CSIRO Division of Marine Research, Marmion WA 6020: [alan.pearce@marine.csiro.au](mailto:alan.pearce@marine.csiro.au)

<sup>2</sup> Centre for Water Research, University of Western Australia Nedlands, WA 6907: [pattiar@cwr.uwa.edu.au](mailto:pattiar@cwr.uwa.edu.au)

Manuscript received February 1997

## Abstract

Satellite remote sensing is the only feasible means of monitoring on a regular basis the large expanse of oceanic surface waters off Western Australia, and marine scientists are increasingly applying this technology to studies of our coastal and ocean waters. Up to now, most use has been made of Landsat Multi-Spectral Scanner (MSS) and Thematic Mapper (TM) imagery for studies of estuarine and coastal features, and the NOAA Advanced Very High Resolution Radiometer (AVHRR) for sea-surface temperature and inferred ocean currents. Some preliminary work has also been undertaken on the chlorophyll distribution of our continental shelf waters using the Coastal Zone Colour Scanner (CZCS). Satellite remote sensing will continue to play an indispensable role in marine science with the availability of altimeters for directly monitoring sea-surface elevations (and hence ocean circulation), scatterometers for surface winds and waves and ocean colour sensors for studies of chlorophyll distributions and ocean productivity.

## Introduction

Western Australia has a coastline of some 8230 km (excluding offshore islands, which increase the total coastline to about 12330 km; R Galloway personal communication) and the area of the continental shelf is about 400,000 km<sup>2</sup> (Jarvis 1986). Because of the complexity of oceanic processes on a range of temporal and spatial scales as well as the expense and limited range of research vessels, the only effective way of monitoring such large areas on a regular basis is through remote sensing. For the past decade, marine scientists in Western Australia have effectively applied satellite remote sensing to study our ocean waters, using the imagery to complement oceanographic data collected by conventional (surface-based) methods and to obtain background information for areas where little other data are available.

Satellite remote sensing has appreciably advanced our knowledge of surface oceanic features off Western Australia. Over the next decade, more accurate and higher resolution satellite sensors will play an increasingly important role in marine research, improving our knowledge of ocean circulation, mixing processes, upwelling systems, wave generation, plankton blooms and fish distributions. It must be remembered, however, that remote sensing effectively covers only the surface waters of the oceans, and therefore complements conventional oceanographic measurements of the subsurface structure.

In contrast with the cool equatorward eastern boundary currents in the South Atlantic and South Pacific Oceans, the dominant ocean current along the Western Australian coast is the Leeuwin Current (Godfrey & Ridgway 1985; Pearce & Walker 1991; Smith *et al.* 1991), a warm poleward flow of tropical water (Fig 1). Also unlike the Benguela and Humboldt Current systems,

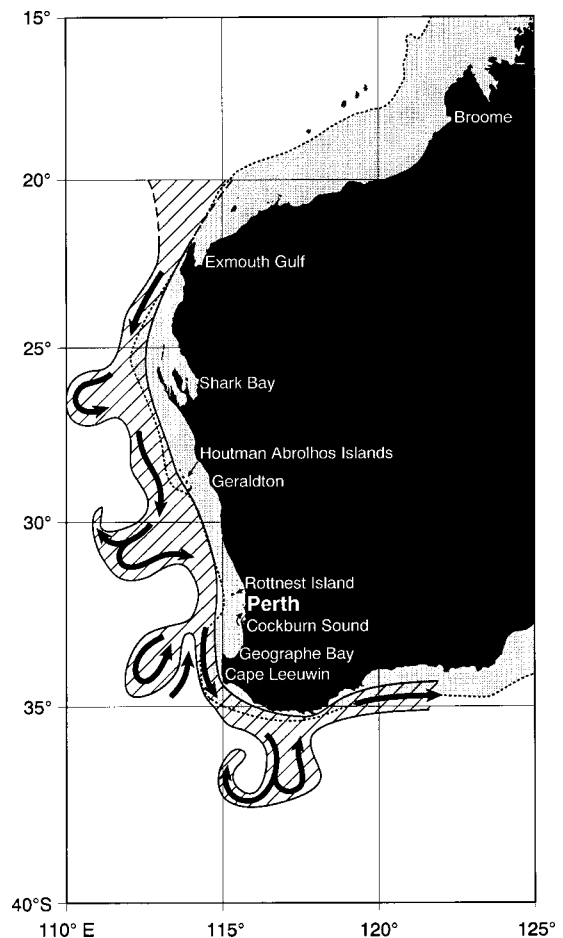


**Figure 1.** Map of Western Australia showing its marine regions. The cross-hatch area is a schematic representation of the Leeuwin Current, and the dotted line shows the approximate position of the edge of the continental shelf.

there is no persistent upwelling of cool nutrient-rich sub-surface water onto the Western Australian continental shelf, and consequently sea temperatures off Western Australia are significantly higher than at the same latitudes off southwestern Africa and Chile (Pearce 1991). The Leeuwin Current appears to play an important role in the biogeography of the south-eastern Indian Ocean (Maxwell & Cresswell 1981; Morgan & Wells 1991; Hutchins & Pearce 1994) and to influence recruitment to some of the commercial fisheries of Western Australia (Pearce & Phillips 1988; Lenanton *et al.* 1991; Fletcher *et al.* 1994; Caputi *et al.* 1995).

Here we review applications of satellite remote sensing in Western Australian coastal and continental shelf waters, briefly outlining the most important results from published as well as unpublished research. Our aim is to demonstrate both the past use and future potential of marine remote sensing in our State and to illustrate how different remote sensing techniques have contributed to our knowledge of local oceanic processes. Technical details should be sought in the standard oceanographic remote sensing textbooks such as Robinson (1985) and Stewart (1985) and in the companion paper by Smith (1997). Further information on local marine applications can be gained from the extensive bibliography prepared by Smith & Pearce (1997).

### Satellite remote sensing

It is less than four decades since the first satellite (the Russian Sputnik) was launched into space in October 1957, to be followed by many earth-observing satellites with a variety of specialised sensors (Fig 2). The "modern era" of oceanographic remote sensing was perhaps born in 1978 when three highly successful satellites were launched; the short-lived Seasat (with a wide array of sensors including an altimeter, synthetic aperture radar SAR and scatterometer), Nimbus-7 (with the Coastal Zone Colour Scanner CZCS) and TIROS-N (carrying the Advanced Very High Resolution Radiometer AVHRR). Satellites may be broadly classified as geostationary (effectively fixed in space some 36000 km above the equator and rotating with the earth) or polar-orbiting.

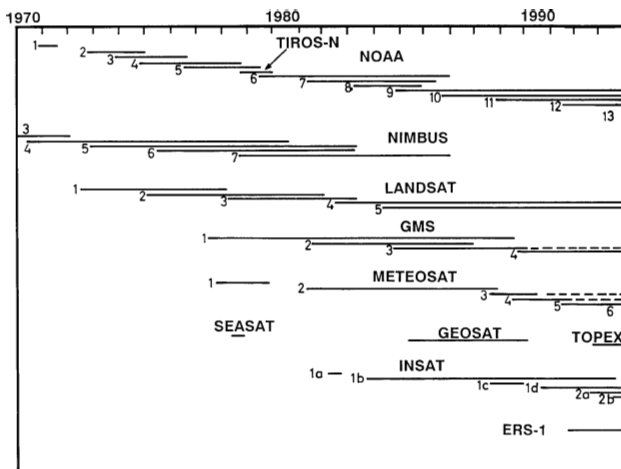


**Figure 2.** Operational periods of selected satellites useful for marine remote sensing from 1970 to 1993. Dashed lines indicate satellites which are still functional but not currently operational. (See text for details.)

There is a chain of geostationary meteorological satellites viewing almost the entire earth's surface at half-hourly intervals; these include the Japanese GMS satellite (located above the equator at 140° E to the north of Australia), the European Meteosat and Indian Insat. These carry both visible and infrared sensors and are largely used for weather monitoring although they have also been used for oceanographic purposes in some parts of the world.

Polar-orbiters, on the other hand, orbit the earth a few hundred km over the poles with a revisit period of one to a few days, and generally have a higher spatial resolution (smaller pixel size on the surface) than the geostationary series. Many of the polar-orbiting satellites have played a crucial role in oceanography, including the highly successful TIROS/NOAA meteorological satellites (with altitudes around 830 to 870 km and orbital periods of about 102 minutes, first launched in the late 1970s and providing more useful imagery over the oceans than any other series of satellites) and the Landsat series, launched in June 1972 as the first operational high-resolution satellite monitoring the earth's surface and resources. Nimbus satellites generally carried experimental sensor packages which may have then become operational on other satellites. Seasat and Geosat were specialised satellites for monitoring sea-surface topography and roughness, as are the currently-operating Topex/Poseidon and the European Remote Sensing Satellite ERS-1.

There are four basic properties of the ocean which can be measured using the visible, infrared and microwave portions of the electromagnetic spectrum. These are:

- surface temperature, which reveals surface circulation patterns including thermal fronts and upwelling zones;
- water colour, used to measure phytoplankton and other particulates in the water column as well as properties of the seabed, and so assist in the study of ocean fronts, surface circulation patterns, upwelling regions, dispersion of river and outfall effluent plumes, and seabed habitats in shallow water;
- surface elevation, where microwave altimeters measure the distance between the satellite and the sea surface to study ocean circulation and tidal heights; and
- surface roughness, showing surface waves and wind from backscatter caused by wind on the ocean surface.

The first two properties can be measured using passive techniques in which electromagnetic radiation emitted by (or reflected from) the water surface and the atmosphere is received at the satellite sensor. The third and fourth properties are measured by the return of pulses of electromagnetic energy that are actively transmitted from the satellite and the reflected/scattered signals are received back at the sensor.

For larger-scale oceanic studies, such as mesoscale (10's to 100's of kilometres) ocean circulation and monitoring of upwelling zones, the polar orbiters with sensors such as the AVHRR and CZCS (pixel size of order 1 km) are adequate. For coastal waters, where smaller-scale processes are important, sensors such as the Landsat TM with pixel sizes of less than 100 m are appropriate.

We concentrate here on satellite remote sensing of surface temperature and ocean colour in Western Australian waters to illustrate the role that each has played (or is playing) in studying marine systems in this State. Satellite measurements of surface topography and roughness have not yet been used to any extent in our waters but will almost certainly become invaluable tools in the future.

### Sea surface temperature

Satellite-derived sea-surface temperature (SST) measurements have been available for over two decades and have been widely used for the derivation of circulation patterns, structure of oceanic fronts, behaviour of eddies/meanders and the location of upwelling zones. The temperature in the upper layer of the ocean is influenced by radiative processes and both incoming and outgoing surface heat fluxes. Vertical mixing usually ensures that the temperature of the thin surface "skin" (from which the infrared radiation is emitted) is close to the "bulk" temperature of the upper few metres of water. Surface temperatures therefore generally reflect the subsurface thermal structure which is in turn related to ocean currents.

SST can be estimated using thermal infrared sensors such as the AVHRR on the NOAA series of satellites, with a pixel size of 1.1 km and a swath width of about 2800 km (Fig 3) and the Thematic Mapper (TM) on

Landsat 4 and 5, which has a single thermal infrared channel with 120 m pixels and a 185 km swath. Two NOAA satellites are maintained operationally at any time, and each passes over any particular place on the earth's surface twice per day. The AVHRR on satellites NOAA-7, -9, -11, -12 and -14 has 5 spectral bands; one in the visible region of the spectrum, one in the near-infrared, a third in the mid-infrared, and two in the thermal infrared. The visible and near-infrared bands are useful in daylight for land/sea/cloud discrimination, and combinations of these bands are used to derive vegetation indices (Smith 1997) and for cloud detection. Techniques of cloud detection are many and varied, but the simplest (and most popular) involve using threshold limits from both individual bands and combinations of bands (e.g. Saunders & Kriebel 1988a, b).

Sea-surface temperatures are computed by combining the radiance temperatures derived from the two individual thermal bands to account for the varying amounts of water vapour in the atmosphere (Barton 1995). Pearce *et al.* (1989) compared AVHRR-SSTs derived from a variety of SST algorithms with surface measurements off Perth and selected the McMillin & Crosby (1984) formulation as giving the most reliable results in this area; this was confirmed by some unpublished data from the Abrolhos Islands, although on occasion the difference between the AVHRR and *in situ* temperatures was found to exceed 2 °C. [More recent unpublished data indicates that better

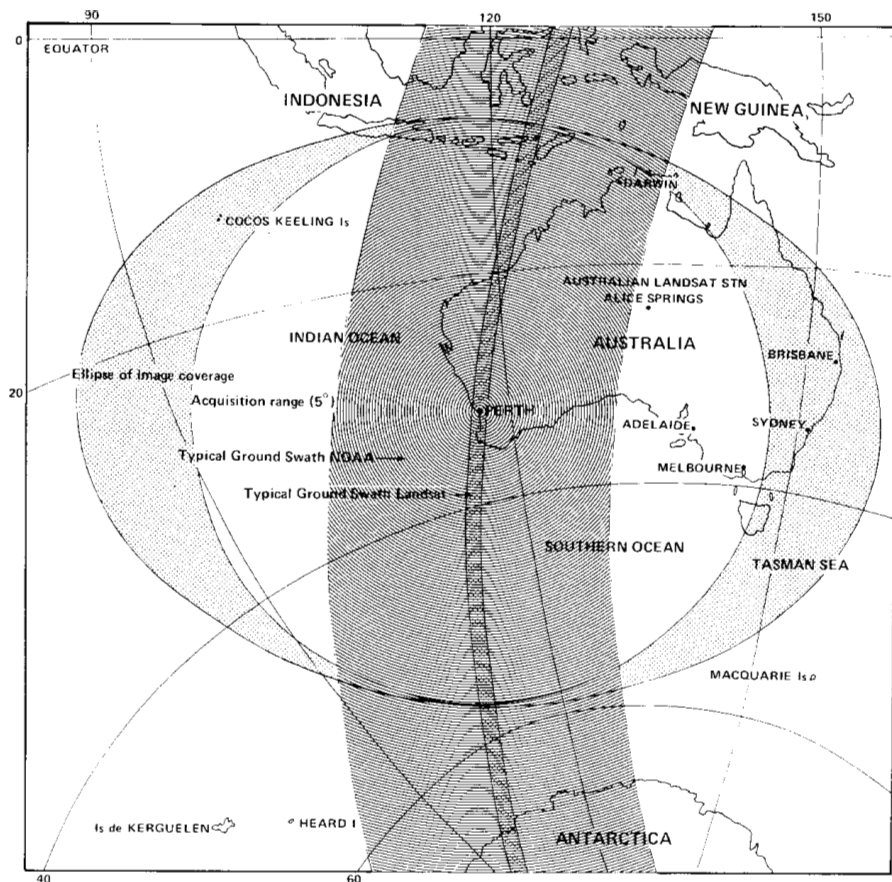


**Figure 3.** Map of the approximate coverage of a typical swath of the NOAA/AVHRR (broad shaded band) compared with that of Landsat (narrow band) (Carroll 1982). The stippled circle/ellipse indicates the total reception area for the AVHRR from the Perth receiving station.

corrections may in fact be required near the edges of the swath, the so-called "scan-angle effect"]. Pellegrini & Penrose (1986) found that the McMillin & Crosby (1984) algorithm was also appropriate for tropical waters of the Northwest Shelf, but they suggested that scan-angle effects may become important towards the edges of images in such regions with high water-vapour loadings.

Western Australian satellite users are fortunate that the first AVHRR receiving station in Australia was established in Perth in 1981 (Carroll 1982) as a joint project between CSIRO and the Western Australian Institute of Technology (now Curtin University). AVHRR satellite images from satellites NOAA-6 to NOAA-14 have been archived in Perth since late 1981, the longest AVHRR archive in Australia (Pearce 1989) which is being used extensively in studies of the Leeuwin Current and its interaction with inner-shelf waters.

#### NOAA/AVHRR: Large-scale circulation and the Leeuwin Current

Historically, the earliest use of SST imagery off Western Australia appears to have been a study of thermal conditions on the Northwest Shelf in 1966 by Szekielida & Mitchell (1972), who used High-Resolution InfraRed (HRIR) imagery from the Nimbus-2 satellite to derive the annual cycle of SST. They also pointed out the presence of anomalously warm patches of water in this region of high air-sea heat flux. Prata & Lynch (1985) and Lynch *et al.* (1986) further examined these patches (which can have a horizontal scale of 200 km and are up to 2° warmer than the surrounding water) and deduced that they can propagate southwestwards at over 1 m s<sup>-1</sup>. This is too fast for normal advective processes, so it was concluded that the patches are possibly caused by spatial and temporal variations in localised heating/cooling of the near-surface waters.

While earlier studies of ocean temperatures and salinities had shown a seasonal change in water properties off Western Australia (Rochford 1969; Gentilli 1972), current trajectories from free-drifting buoys as well as hydrographic measurements led to the identification and naming of the Leeuwin Current (Cresswell & Golding 1980). The advent of NOAA/AVHRR imagery received in the United States in the late 1970s provided the thermal resolution to confirm the strong southward transport down the west Australian coast during the autumn and winter months and the much weaker flow in summer, also revealing details of the complex eddy-like features associated with the Leeuwin Current (Fig 4; Legeckis & Cresswell 1981).

Since the establishment of the NOAA receiver in Perth in 1981, locally-received AVHRR imagery has become a well-used tool in studies of the structure and variability of the Leeuwin Current and associated coastal waters off Western Australia. The surface temperatures show the Leeuwin Current as a strong current meandering southwards from about Exmouth along the edge of the continental shelf; on reaching Cape Leeuwin, it curves eastwards and flows into the Great Australian Bight.

Along both the west and south coasts, however, satellite (Prata *et al.* 1986; Pearce & Griffiths 1991) and drifting buoy (Cresswell 1980) studies have shown that the Leeuwin Current is in fact a complex of mesoscale (order of 100 km) eddies and meanders interposed with along-

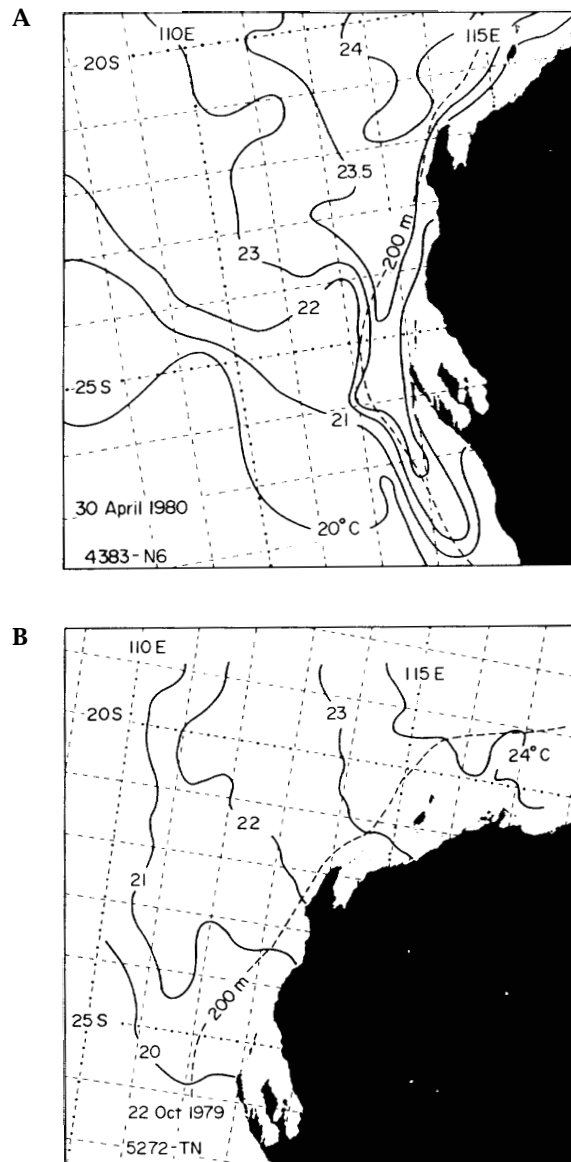
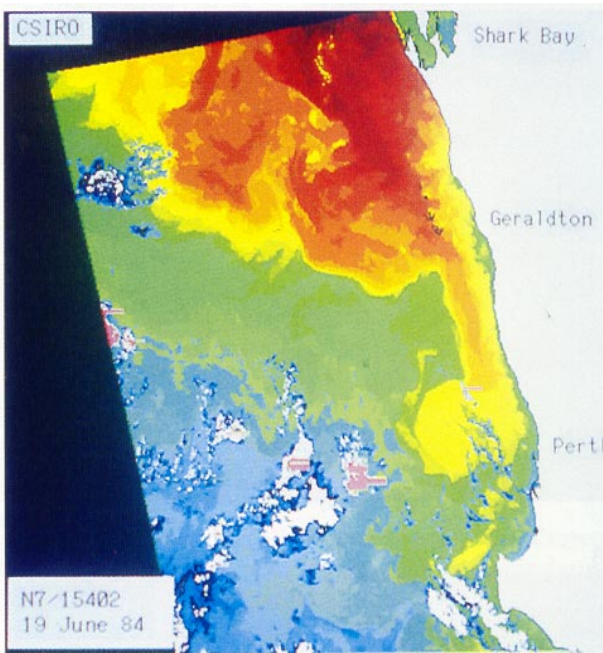


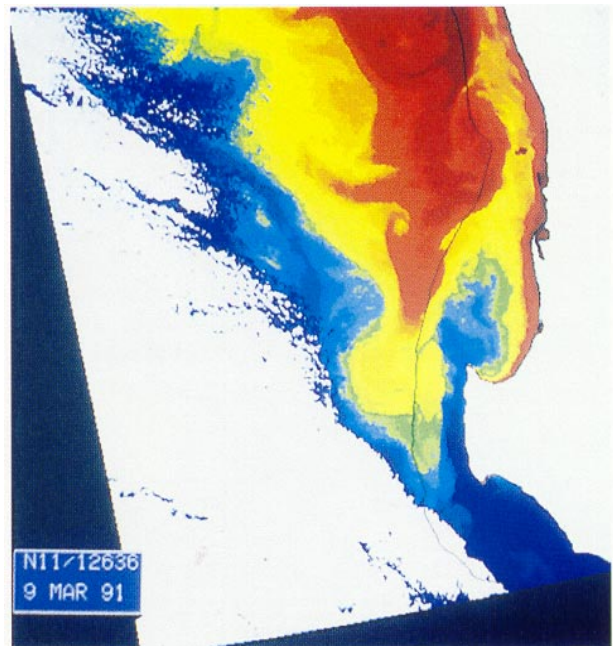
**Figure 4.** Sea-surface temperature contours off Western Australia. **A:** April 1980, the tongue of warm water penetrating southwards along the outer continental shelf showing a strongly-flowing Leeuwin Current. **B:** October 1979 with a weak current. Reprinted from Deep-Sea Research Volume 28, Legeckis R & Cresswell G R, Satellite observations of sea-surface temperature fronts off the coast of western and southern Australia, pages 297-306. Copyright 1981. With kind permission from Elsevier Science Ltd, The Boulevard, Langford lane, Kidlington OX5 1GB, UK.

shore current jets. There are frequently a number of these wave-like meanders of different dimensions along the west coast, deflecting the Current offshore and representing an active transport of warm Leeuwin Current waters into the southeast Indian Ocean (Plate 1). These anti-cyclonic (anti-clockwise) meanders can grow to more than 200 km from the coast on occasion before apparently becoming unstable and either breaking off as free-standing eddies (Griffiths & Pearce 1985a) or simply dissipating. Between the meanders, strong alongshore current jets stream southwards along the shelfbreak and outer continental shelf.

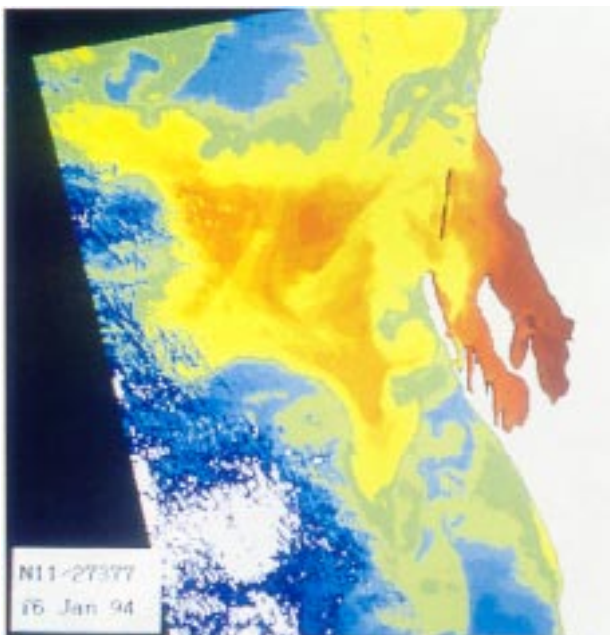
1



2



3



4

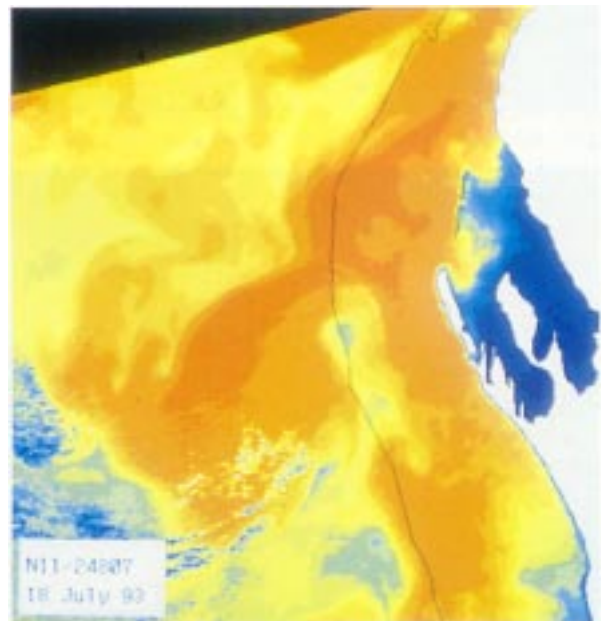


**Plate 1.** NOAA-AVHRR image of the Leeuwin Current between Shark Bay and Cape Leeuwin in June 1984. The image has been geometrically corrected and shows the brightness temperature in band 4, with warmest water (the Leeuwin Current) in red cooling through yellow and green to the coldest water in blue. Land is white and clouds are mottled blue/white. Image received by the Western Australian Satellite Technology and Applications Consortium.

**Plate 2.** NOAA-AVHRR image of the cool Capes Current flowing northwards off south-western Australia in March 1991. Other details as in Plate 1.

**Plate 3.** NOAA-AVHRR image of Shark Bay; January 1994, representing summer conditions. Other details as in Plate 1.

**Plate 4.** NOAA-AVHRR image of Shark Bay; July 1993, for winter. Other details as in Plate 1.

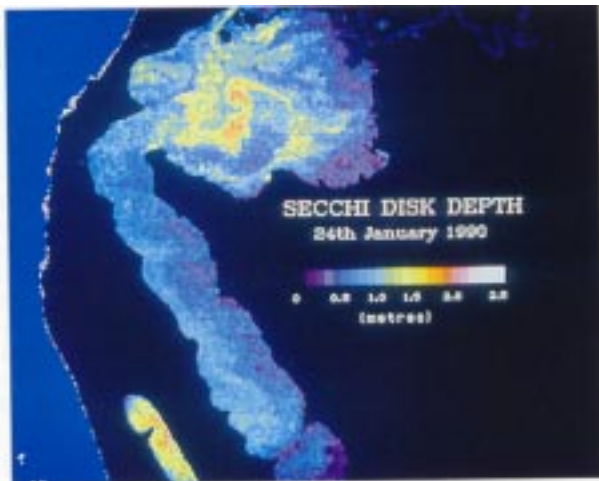
5



6



7



8



**Plate 5.** Bathymetry off Broome derived from a Landsat TM Band 1 image in December 1987. The image shows bottom stratigraphic features, the two features parallel to the coast in the middle of the picture being in water depths of 15 to 30 m. (Image courtesy of Peter Hick, CSIRO).

**Plate 6.** Wake eddy behind Cape Voltaire ( $14^{\circ} 16' S$ ,  $125^{\circ} 35' E$ ) in Admiralty Gulf, enhanced from a Landsat TM image. The horizontal scale of the eddy is about 1 km in a current of about  $1.5 \text{ m s}^{-1}$ .

**Plate 7.** Landsat TM image of the Peel-Harvey estuary, showing the equivalent of Secchi disk depth on 24 January 1990, derived from a combination of Landsat TM bands 1 and 3. Reprinted by permission of the Publisher, from Lavery P S, Pattiaratchi C B, Wyllie A & Hick P T, Water quality monitoring in estuarine waters using the Landsat Thematic Mapper, Remote Sensing of Environment Volume 46 pages 268-280. Copyright 1993 by Elsevier Science Inc.

**Plate 8.** Landsat MSS composite image (bands 4, 5, 7) of the Capes area on 14 November 1984 (courtesy Alex Wyllie and Robert Shaw, WA Department of Land Administration) showing internal waves near Cape Leeuwin.

Closer inshore, there is a seasonally-varying northwards counter-current along the continental shelf north of Rottnest Island (Cresswell *et al.* 1989). However, satellite images have suggested that a cold plume also penetrates northwards past Cape Leeuwin during the summer months (Phillips *et al.* 1991; Cresswell & Peterson 1993). More detailed analysis of a series of AVHRR images enabled Pearce & Pattiaratchi (unpublished observations) to define and name the Capes Current, a nearshore current flowing northwards past Capes Leeuwin and Naturaliste and along the mid-continental shelf past Rottnest Island. In contrast with the winter situation where the Leeuwin Current is close inshore near Cape Leeuwin, the Leeuwin Current swings offshore in summer as the Capes Current penetrates northwards against the coast (Plate 2). This cool current (which may also involve localised upwelling; Gersbach *et al.* personal communication) is narrow and shallow, persisting between about October and March while the wind stress is strongly northward.

After rounding Cape Leeuwin, the Leeuwin Current changes character. In contrast with the meandering behaviour along the west coast, where the current path as a whole deflects offshore, the current along the south coast tends to run along the outer continental shelf (with the strongest currents just beyond the shelfbreak) towards the Great Australian Bight. It is characterised by strong thermal fronts as the tropical water borders cold Southern Ocean waters. Periodically, warm offshoots peel off to the south and temporarily disrupt the eastward flow (Griffiths & Pearce 1985b; Cresswell & Peterson 1993); these features frequently have the form of eddy pairs, with clearly-defined clockwise (cool) and anticlockwise (warm) circulation elements. Some offshoots continue

growing southwards away from the coast and eventually separate from the Current to drift away as freely-rotating eddies 300 km or more offshore (Griffiths & Pearce 1985a).

Using AVHRR imagery to complement simultaneous Acoustic Doppler Current Profiler (ADCP) measurements from a research vessel, the three-dimensional structure of the Leeuwin Current and some of the warm offshoots can be analysed. Cresswell & Peterson (1993) measured current velocities in some of the offshoots which were evident in satellite images, finding current speeds of up to  $1.5 \text{ m s}^{-1}$  (Fig 5). This work is a fine example of the value of linking conventional oceanographic measurements with satellite imagery.

By extracting digital SST transects across the Leeuwin Current from the imagery, the surface expression of the current structure can be quantified in terms of the position of the peak temperature in the current and derivation of SST gradients (Prata & Wells 1990; Pearce & Griffiths 1991). The thermal topography varies seasonally and with latitude. During the summer months when the Leeuwin Current is weak, the thermal structure is ill-defined and SST gradients are small, but significantly increase while the current is strengthening in autumn, before decaying again in late spring (Pearce & Prata 1990). As the Leeuwin Current flows southwards into increasingly cool waters, the temperature differential across its boundary correspondingly increases. At the latitude of Shark Bay, this differential is typically about  $1^\circ \text{ C}$ , whereas off Perth it is more like  $2^\circ$  to  $3^\circ \text{ C}$  and along the western part of the south coast where the warm Leeuwin Current waters enter the Southern Ocean it can exceed  $4^\circ \text{ C}$  (Godfrey *et al.* 1986; Prata & Wells 1990).

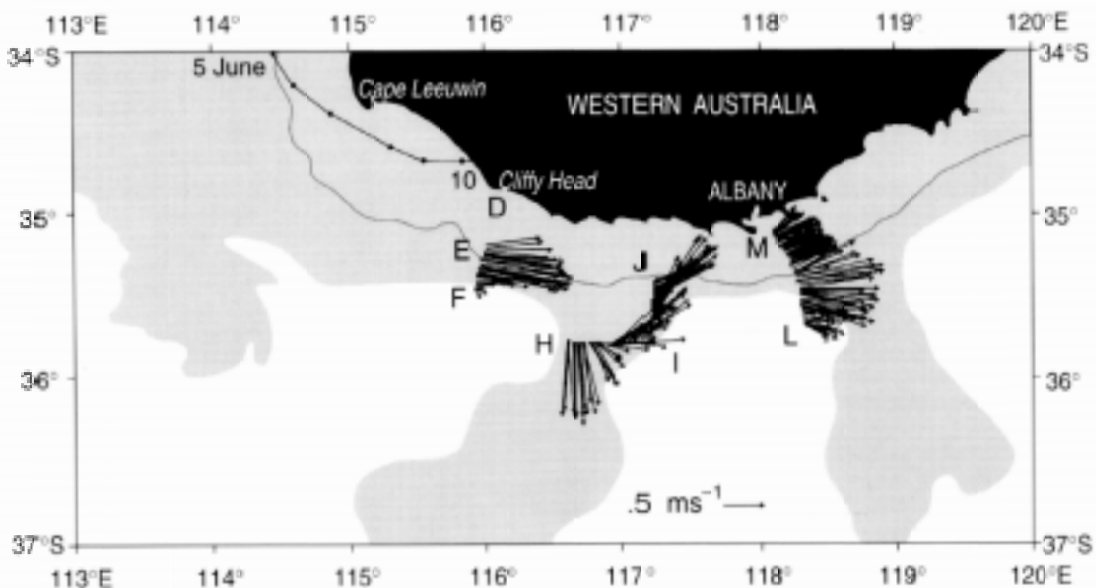


**Figure 5.** Surface currents in Leeuwin Current offshoots along the south coast near Albany. The shaded region represents warmer water from a NOAA-AVHRR image and the current vectors are from the ADCP (see text). The letters D to L are from the original paper and are not used here. Reprinted by permission of the Publisher from Cresswell G R & Peterson J L, The Leeuwin Current south of Western Australia, Australian Journal of Marine and Freshwater Research Volume 44 pages 285-303. Copyright 1993.

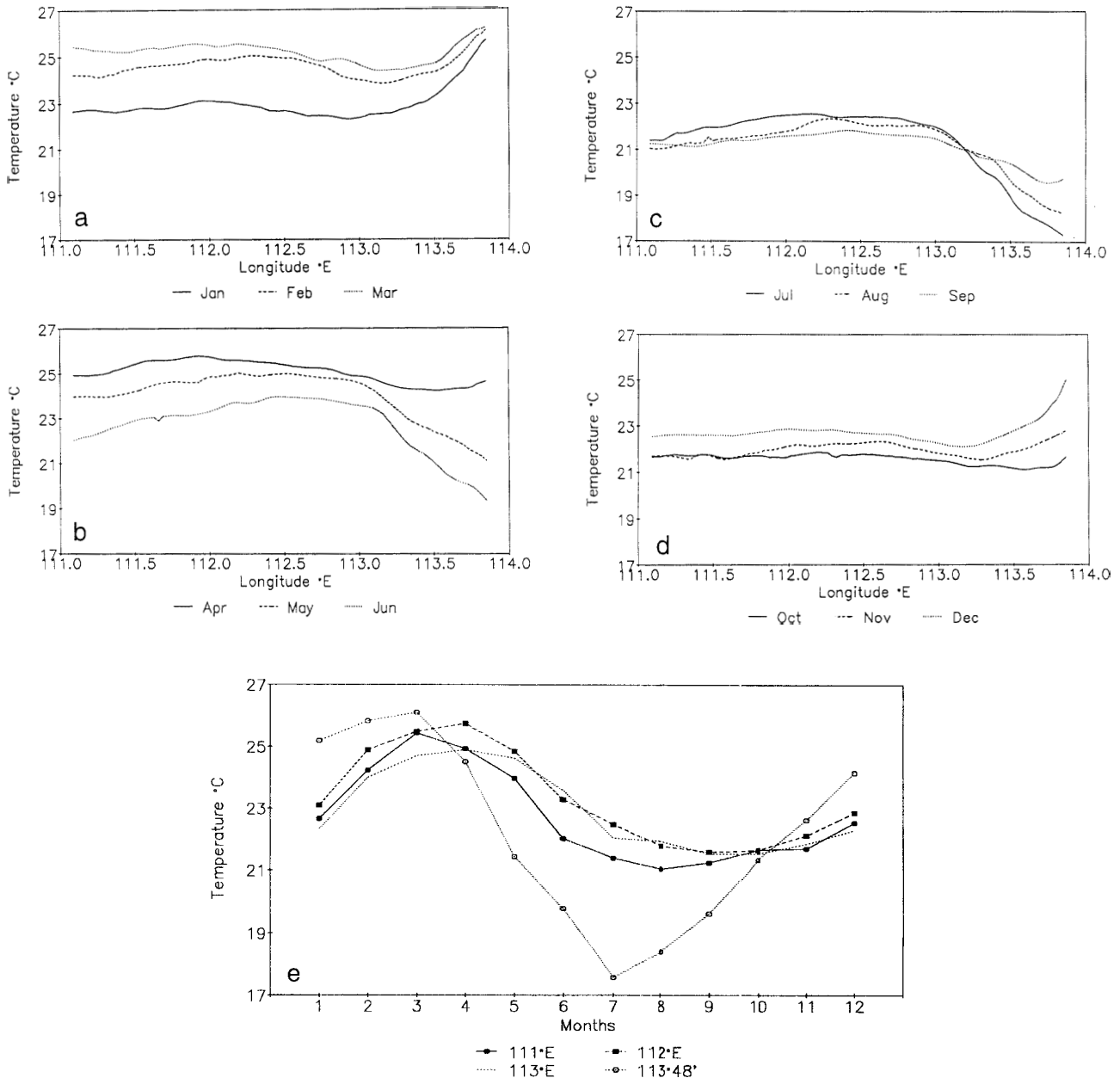


**Figure 6.** A to D Monthly mean SST transects on latitude 25° 20' S across the continental shelf between 111° E and the eastern shore of Shark Bay derived from AVHRR data 1988 to 1993. E: depicts the seasonal SST cycle at four selected longitudes representing offshore water (111° E), the Leeuwin Current (112° E), the entrance to Shark Bay (112° E) and the shallow eastern part of Shark Bay (113° 48' E).

Prata *et al.* (1986) derived the trajectory of the Current by determining the position of the peak SST along each dataline, clearly illustrating the meandering of the flow down the coast.

Another example of digital data extracted from AVHRR imagery is a series of monthly mean SST transects across the continental shelf at 25° 20' S and extending into Shark Bay, illustrating the seasonal variation in cross-shelf thermal structure. In the summer months (Fig 6A, Plate 3), the water near the eastern shore of Shark Bay is 3° to 4° C warmer than that outside the Bay. During autumn and into winter (Plate 4; Fig 6B, C), the shallow water in the bay cools as heat is lost to the

atmosphere so that by June the eastern bay water is 4° C cooler than that in the Leeuwin Current. As spring extends into summer, the cross-shelf gradient switches again (Fig 6D). The transition months when the water is almost isothermal across the shelf and Bay are April and October. The seasonal variation is graphically shown in Figure 6E where both the amplitude and phase of the annual cycle change between offshore and the bay itself; in the Leeuwin Current (112° E) the water is warmest in May and coolest in September/October and the annual range is 4° C, whereas in the eastern bay (113° 48' E) the range is almost 9° C and the extremes are in March and July.

### NOAA/AVHRR for fisheries applications

Because of anticipated links between water temperatures and fish catches (particularly for pelagic species such as tuna), one of the original motivations for establishing the NOAA remote sensing facility in Perth was to provide SST imagery to the fishing industry. A study examining the correlation between satellite-derived SSTs (provided in real-time to the fishing industry) and southern bluefin tuna catches along the southwestern coast of Australia (Myers & Hick 1990) found somewhat inconclusive results. This was largely because of the inadequate facilities available for image acquisition and processing at that time, persistent cloud over the fishing area near Albany, the general decline of the tuna stock (with consequent changes in the operation of the industry) and the practices of the fishermen themselves. Nevertheless, recent improvements in both the reception and image processing facilities have enabled SST images to be made available to the fishing industry in real-time, and some fishing companies in Western Australia are now making use of the pictures to assist in fishing management decisions.

To explain some of the established links between the flow of the Leeuwin Current (as indexed by annual mean coastal sea levels) and recruitment of the western rock lobster, Pearce & Phillips (1988) have suggested that the strong onshore flow in the southern part of mesoscale meanders may regionally boost the shoreward migration of the phyllosoma larvae. A particularly well-defined meander in an AVHRR image during the settlement period in October 1984 may have contributed to exceptionally high local settlement at Dongara at that time. Likewise, AVHRR images suggested that fluctuations in recruitment at Cape Mentelle (34° S) may be associated with the onshore/offshore position of the Leeuwin Current in that area (Phillips *et al.* 1991).

The annual recruitment of tropical fish larvae at Rottnest Island in April has been attributed by Hutchins & Pearce (1994) to the southwards flow in the Leeuwin Current. Analysis of AVHRR imagery indicated that the arrival of larvae was associated with tongues of Leeuwin Current water penetrating across the shelf to bathe the Island, although the authors acknowledged that other factors (both oceanographic and biological) would certainly play a role as well.

Fletcher *et al.* (1994) used AVHRR images to assist in the interpretation of pilchard larval and egg distributions along the south coast. Larval surveys during the July spawning period when the current flows most strongly showed that there was eastward advection of eggs and larvae along the shelf at between 30 and 40 km d<sup>-1</sup> (35 to 45 cm s<sup>-1</sup>). During the December spawning, on the other hand, there was no indication of alongshore advection of eggs and larvae because the current is weaker at that time of year.

AVHRR imagery also proved useful in explaining the movement of an oil slick from the tanker Kirki which lost its bow near Jurien in 1991, with fears that the oil spill could decimate the sensitive rock lobster nursery reefs. Analysis of SST images shortly after the disaster showed that a meander of the Leeuwin Current was responsible for carrying the oil offshore despite generally onshore winds at the time. Use of current patterns derived from

the imagery in OSSM (the On-scene Oil Spill Model) enabled the oil distribution to be reproduced in the model (Easton *et al.* 1992), proving the value of satellite imagery in marine disasters of this type.

### NOAA/AVHRR and submerged strandlines

In a novel use of AVHRR thermal imagery, Tapley (1990) produced a relief-shaded night-time image of surface thermal boundaries for a coastal region off Broome. Oceanic eddies were revealed, but more surprisingly the image also showed the surface expression of submerged limestone strandlines consisting of pairs of narrow ridges some 300 to 500 m wide and rising 5 to 8 m above the seabed in water about 20 m deep. Tapley's interpretation was that the strandlines created vertical currents and both the upwelled cooler water and changed surface sea-state were evident as a thermal signature. The presence of the strandlines was verified by diver observations during the validation phase of the study.

### NOAA/AVHRR for coastal processes

While the mesoscale meanders and eddies described above extend offshore (westwards), smaller eddies and billows with length scales between 5 and 35 km are also found along the inshore boundary of the current and penetrate across the continental shelf (Pearce & Griffiths 1991; Wyllie *et al.* 1992). Field studies of nearshore oceanographic processes off Perth using conventional oceanographic measurements complemented by NOAA-AVHRR and Landsat TM imagery have revealed some of the dynamics of the interaction between the Leeuwin Current and the nearshore waters (Mills *et al.* 1992). Cross-shelf mixing processes result in active "flushing" of the inshore region and are believed to play a role in the dispersal of coastal pollutants. A composite TM image also showed discoloured water from the Peel-Harvey estuary and the Swan River moving northwards (Wyllie *et al.* 1992), illustrating the complementary roles of multi-spectral and multi-scale imagery in interpreting coastal and nearshore processes.

Nevertheless, under appropriate conditions NOAA/AVHRR imagery alone can reveal relatively small-scale localised features, such as upwelling around Rottnest Island caused by the interaction between flow and topography ("island wake effect"). During the summer months, the predominantly southerly winds drive the currents on the continental shelf northward past Rottnest Island, resulting in a persistent cold water patch immediately to the north of the Island (Pattiaratchi, unpublished data). During winter, on the other hand, interaction between the southward flowing Leeuwin Current and Rottnest Island leads to flow separation with the formation of an eddy off the western tip of the Island.

Another coastal application of full-resolution thermal AVHRR imagery involved a tidal jet from an estuary at Bunbury (Hearn & Pearce 1985), showing a plume of buoyant warm water extending some 5 km from the inlet, with a maximum thermal contrast of about 0.5° C; this is approaching the limits of the radiometric and spatial resolution of the AVHRR sensor. Estimates of the frontal propagation speed and entrainment coefficient using the image and a tidal model agreed with those obtained using surface measurements.

## Ocean Colour

In contrast with thermal infrared remote sensing, comparatively few ocean colour data are available for Western Australian continental shelf waters, because the CZCS was operational only intermittently and because the visible band on the AVHRR has insufficient spectral resolution to adequately detect the small range of colour changes in the open ocean. For coastal waters, however, remote sensing in visible wavelengths has been used for monitoring chlorophyll (phytoplankton) concentrations, suspended sediments, and bottom type (in clear shallow water). Visible imagery is, of course, only useful during daylight hours and in cloud-free conditions.

While thermal infrared energy is emitted from a thin surface skin, water-leaving radiance in the visible region of the spectrum indicates colour variations in the upper part of the water column, depending on the absorption, reflection and scattering of sunlight from particles in the water as well as on surface illumination, roughness, foam and surface films. Clearly, the spectral characteristics of a water body depend markedly on the mix of phytoplankton species present, the ages of the various components and the presence of inorganic particles. Because much of the radiance reaching the satellite is from scattering and reflection by the atmosphere, corrections must be applied to remove these atmospheric components from the water-derived upwelling signal.

The colour sensors which have been most widely used are the Multi-Spectral Scanner (MSS) and the Thematic Mapper (TM) on the Landsat series of satellites, and the Coastal Zone Colour Scanner (CZCS) which operated between 1978 and 1986 on the experimental Nimbus-7 satellite. The CZCS was the first satellite sensor dedicated to monitoring phytoplankton and sediments in the near-surface waters of the ocean. The bands had narrow bandwidths and high sensitivity tailored to the absorption spectrum of oceanic planktonic pigments, so that chlorophyll concentrations could be determined from the ratios of the radiances in different spectral bands, showing regional and temporal variations in phytoplankton concentration. The CZCS swath-width was about 1600 km and the pixel size 825 m. The Landsat sensors were primarily designed for land applications, but the TM (which has a spatial resolution of 30 m and swath width of 185 km) has proved useful in coastal and bathymetric studies. SPOT is a French satellite with even higher resolution visible sensors (but correspondingly narrower swath) covering similar wavelengths to the Landsat MSS.

The Sea-viewing Wide Field-of-view Sensor (SeaWiFS), scheduled for launch in mid-1997 will provide colour imagery in 8 spectral bands to reveal regions of enhanced biological productivity such as upwelling zones. There have been many unfortunate delays in the launch of this sensor, which will have a swath-width of 2800 km and a resolution of 1.1 km (similar to the AVHRR) and is expected to provide a major boost to coastal oceanic and fisheries-related studies. The Ocean Colour and Temperature Scanner (OCTS) was recently launched on the Japanese Advanced Earth Observing Satellite (ADEOS); it has 8 bands in the visible and near infra-red and 4 in the thermal region of the spectrum, providing coincident visible and thermal imagery with a spatial resolution of about 700 m.

## Landsat TM: Bathymetric and habitat mapping

Because visible radiation can penetrate into the water column, the bathymetry and texture of the seabed can be determined under suitable conditions. The shorter wavelengths at the blue-green end of the spectrum can penetrate deeper than the longer (red) wavelengths, so Landsat TM band 1 (0.45 to 0.50  $\mu\text{m}$ ) is suited to bathymetric determination while band 2 (0.50 to 0.59  $\mu\text{m}$ ) can provide information on the characteristics of the water column. Light reflected from the seabed passes through the water column (where some absorption and scattering by phytoplankton and sediment particles occurs) and then through the atmosphere (with further absorption and scattering) before reaching the satellite sensor. Use of TM imagery for seabed mapping therefore requires the radiances from these component paths to be separated.

Landsat TM imagery has been used to map the seabed in coastal waters off Broome, in Shark Bay, around the Houtman Abrolhos Islands, an area south of Geraldton, in Cockburn Sound and Geographe Bay (Fig 1). The study off Broome examined the relationship between reflectance and depth as well as the spectral reflectance characteristics of pearl oyster habitat (Hick & Scoones 1990). Comparison of data from TM band 1 with hydrographic charts showed that the radiance in this band is highly correlated with bottom depth down to depths approaching 30 m provided the seabed is reasonably uniform, the water clear and the sun high in the sky to provide good illumination conditions. Classification of the substrate in the imagery as reef, sand and seaweed agreed well with visual observations by divers. Plate 5 shows the bathymetric features off Broome, the visible bottom structures being ancient coastlines and wave-cut platforms in water depths exceeding 30 m.

The problem of separating in-water and seabed reflectances has been addressed by Bierwirth *et al.* (1993) using Landsat TM bands 1, 2 and 3 to "unmix" these components in part of Shark Bay (Fig 1), thus providing information on the colour and structure of the seabed as well as estimating the water depth. By assuming a model of the attenuation of radiant flux with depth and the spatial uniformity of suspended materials in the water column, and then applying a constraint to the substrate reflectances for each pixel, both the water depth and bottom type (seagrass meadows, microbial mats and sand) could be determined from the multispectral data.

The distribution of marine habitats at the Houtman Abrolhos Islands has been examined using Landsat TM (bands 1 to 3) and SPOT imagery (Anon 1993, 1994). A number of habitat categories (including sand shallows, coral, seagrass beds and plant-dominated reefs) with different spectral properties were identified from the imagery, aided by aerial photography and diving surveys. Although interpretation of the imagery was ambiguous in waters deeper than 10 to 15 m, it was concluded that the TM and SPOT imagery was useful in providing broad habitat distributions and some new features of the seabed were revealed.

Landsat TM data were also used by Catalano *et al.* (1991) in a study of environmental information for the management of coastal developments (specifically the tourism and fishing industries) along the west coast between

Guilderton and Dongara, south of Geraldton (Fig 1). Mapping of coastal bathymetry to depths of about 10 m, and bottom habitat type was undertaken using Landsat TM bands 1 to 3. While some difficulties were encountered in distinguishing seagrass beds from deeper water and reef systems, and attempts to derive the coastal water circulation were unsuccessful, it was concluded that the use of remotely sensed data showed great potential. However, existing data and/or fieldwork are required to validate interpretation of the satellite information.

Following an earlier study by Gee & Forster (1984) in the moderately turbid waters of Cockburn Sound just south of Perth (Fig 1), Corner & Lodwick (1992) made use of residual modelling to enhance the accuracy of TM depth estimates in waters covering a depth range of 0.3 to 22 m. They found that, under some conditions, the depth estimates could be improved using a calibrated regression relationship between the TM estimates and the surveyed depths (from a chart). Similarly, seabed features in Geographe Bay (Fig 1) could be identified in TM band 1 images at depths down to 45 m under good conditions (Hick *et al.* 1994) using *in situ* radiometric measurements to quantify the effects of suspended sediments and chlorophyll in the water column. The decline in the density of seagrass meadows with increasing depth was evident, as were areas of bare sand where storm events had completely eroded the seagrass.

A wide-ranging description of underwater features (seagrass meadows, reefs, bare sand and deltaic areas) in Western Australia is being undertaken to prepare a national atlas to aid in coastal management (H Kirkman, personal communication). Landsat TM band 1 imagery is being used to prepare maps at a scale of 1:100,000, supported by ground truth observations to confirm features identified in the imagery.

#### Landsat TM: Island wakes

Small-scale dispersion of coral spawn from reefs is assisted by turbulent wakes and eddies shed from the islands or reefs. Landsat TM imagery has been used to study these wakes behind islands and headlands in Admiralty Gulf, Northwestern Australia, where suspended sediment is visible as a tracer (Pattiaratchi 1994). The structure and behaviour of the wakes depends on an "island wake parameter" involving the size of the island, the regional current speed, the water depth and the vertical eddy viscosity coefficient. Analysis of island wakes and headland eddies identified from satellite data has shown good agreement between the observed wakes and those predicted using the island wake parameter. Plate 6 shows a headland eddy shed from Cape Voltaire in Admiralty Gulf observed in a Landsat TM image; the tidal range in this area is up to 6 m at spring tides, which results in maximum surface currents of  $1.5 \text{ m s}^{-1}$  and recirculating eddies with dimensions consistent with the theory.

#### Landsat TM: Water quality

Routine monitoring of water quality parameters such as chlorophyll, suspended sediment, light attenuation, *etc.* in coastal waters may be undertaken using Landsat TM data, and techniques to undertake such studies have been developed for Western Australian estuaries and coastal waters by Lavery *et al.* (1993) and Pattiaratchi *et al.*

(1992). Estimates of the surface chlorophyll concentration and Secchi disk depth (a measure of water clarity) were obtained using the satellite-received radiance corrected for atmospheric effects. The algorithms were developed using water quality data collected at the time of the satellite overpass. The study sites selected were the Peel-Harvey estuarine system (between Perth and Geographe Bay, Fig 1) and Cockburn Sound, two areas where degradation of water quality has been documented over the past few years. The distribution of Secchi disk depths in the Peel-Harvey system derived from a Landsat TM image during a flooding tide clearly showed the frontal structure of the clearer oceanic water (larger Secchi disk depths) and the more turbid estuarine waters (Plate 7).

#### Landsat MSS: Internal waves

An interesting application of Landsat MSS Band 6 imagery was the identification of internal waves on the Northwest Shelf (Baines 1981). Internal waves exist in the interior of the ocean and tend to form along the interface between layers of fluid of different densities. Associated with these waves are surface bands of convergence and divergence (Robinson 1985) with differing surface roughness visible in satellite imagery. They generally lie parallel to bathymetric features. Baines (1981) interpreted the rough/smooth bands on the sea surface as indicating the presence of tidally-generated internal waves on the thermocline with wavelengths of 300 to 1000 m and propagation speeds of between  $0.5$  and  $1 \text{ m s}^{-1}$ .

A more recent (November 1984) Landsat MSS image of the area near Cape Leeuwin has revealed a series of internal waves presumably propagating shorewards from about the position of the continental shelf break, with a wavelength of about 3.5 km (Plate 8).

#### CZCS: Coastal productivity

The only application of CZCS imagery off Western Australia to date appears to be that of Pattiaratchi *et al.* (1990) who used chlorophyll concentrations derived from the CZCS colour bands and SST from the thermal band to examine the interaction between the Leeuwin Current and the continental shelf waters between Shark Bay and Perth (Fig 1). Chlorophyll concentrations were estimated using standard CZCS algorithms with the removal of atmospheric effects.

Although the absolute chlorophyll concentrations were somewhat uncertain, it was clear that the continental shelf waters contain higher chlorophyll levels than in the Leeuwin Current (Pattiaratchi *et al.*, unpublished observations). Mesoscale meanders sweeping the Leeuwin Current onto the continental shelf were evident in the thermal images, matched by the chlorophyll which acted as a tracer indicating that the current was entraining the productive shelf waters and effectively exporting them offshore (Fig 7). Depending on the degree of entrainment, some offshore meanders/eddies were relatively rich in chlorophyll, with implications for enhanced biological production in these water bodies. SST and chlorophyll transects across the eddies clearly showed the entrainment of the chlorophyll-rich shelf waters into one of the eddies.

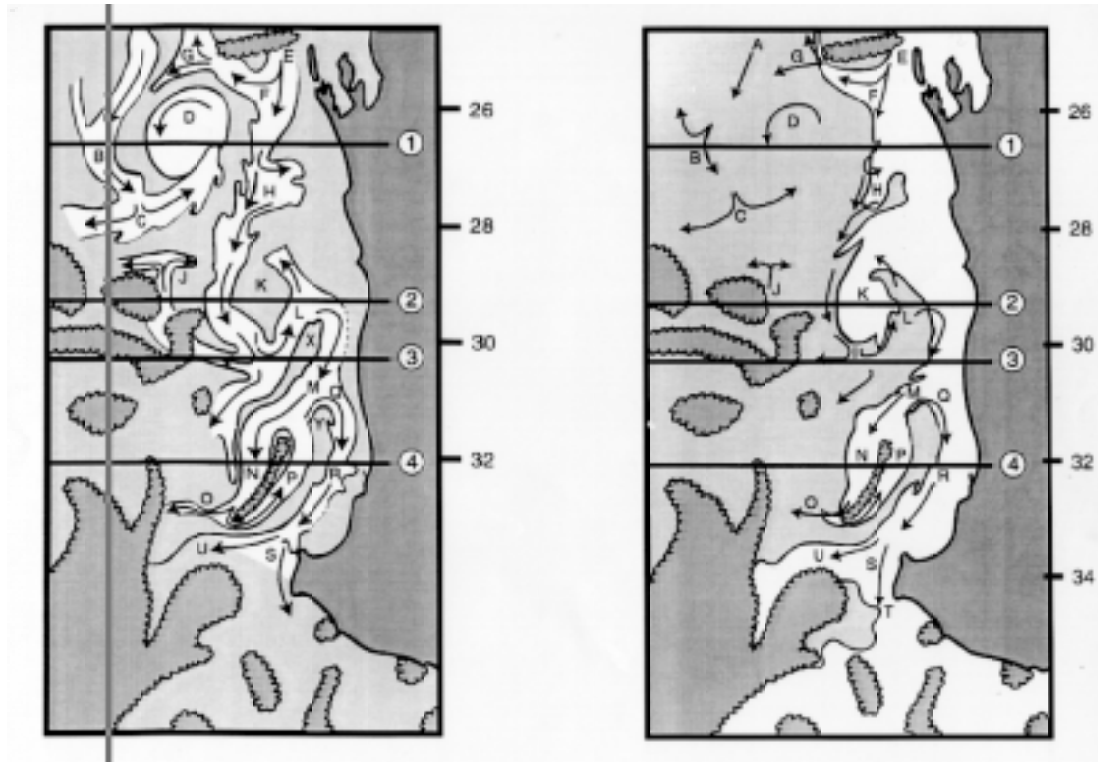


**Figure 7.** Line sketch interpretations of the Leeuwin Current from (A) CZCS thermal infrared image (band 6) and (B) chlorophyll distribution on 10 May 1981, indicating entrainment of high-chlorophyll shelf waters by the Leeuwin Current. The warm Leeuwin Current is depicted as white in A, as are the relatively high-chlorophyll waters in B. The current arrows have been derived from the SST image A and then transferred to the chlorophyll image B. Features D, K and N-P represent eddies, and the main flow in the Leeuwin Current is along E-H-L-M-N-P-Q-R-S. The densely shaded areas with curly boundaries are clouds. Features A to T and the four transects (solid horizontal lines) are not discussed here.

### The future

Understanding the ocean circulation is fundamental to almost all aspects of marine science including biology, fisheries management and research, shipping operations and climate research. There is a growing awareness of the important role played by the circulation in the life histories of many fish and hence in recruitment to commercial fisheries, and the near-realtime tracking of marine pollutants (for example the movement and dispersion of oil spills) by satellite can provide essential and timely information for fisheries managers and pollution authorities to make decisions about appropriate alleviation measures.

Medium resolution thermal imagery (NOAA/AVHRR SST) will continue to provide useful and accessible datasets for monitoring surface features of the large-scale ocean circulation, but is increasingly being supplemented by ocean surface topography. Traditionally, oceanographers have derived the ocean circulation by computing the dynamic height of the sea surface from temperature and salinity profiles, but measurement of sea surface elevation can now be made on a global scale using satellite altimeters such as Topex/Poseidon to yield direct estimates of ocean currents (Fu *et al.* 1994), with the advantage of not being restricted by cloud cover. The distance between the satellite and the sea surface is measured by the time lapse between radar pulses and the return echoes of a narrow beam transmitted vertically downward from the altimeter to the sea surface. The vertical resolution of

altimetric measurements has steadily improved from about 1 m (Skylab) to about 5 cm (Topex; Fu *et al.* 1994) subject to corrections for uncertainties in the geoid, orbit error, atmospheric and ionospheric effects, errors related to sea state, and tides. Acquisition of global sea level data will also allow monitoring of sealevel variability as a result of climate change. Complementing thermal satellite imagery with ADCP-measured currents has confirmed that, at least in subtropical regions with strong boundary currents, surface temperatures generally indicate near-surface current patterns (Cresswell & Peterson 1993).

Most of our present knowledge of global wind and wave conditions has been derived from shipping observations. Satellites can provide wind and wave data on a regular basis over large areas, including remote and inhospitable ocean regions, by recording the roughness of the ocean surface with instruments such as the altimeter, synthetic aperture radar (SAR) and scatterometer (Stewart 1985). The first satellite to carry all these instruments was the short-lived SeaSat (which operated for only about 3 months in 1978), and they are now on the currently-operational European ERS satellites. Satellite-derived wind and wave estimates from the present generation of satellite instruments are comparable with those using *in situ* measurements and are available for coastal wave climatologies and offshore maritime activities such as oil production, shipping and coastal engineering. Routine monitoring of sea state and winds off Western Australia from satellites is very likely in the near future.

Following the important results derived from CZCS colour imagery, the availability of ocean colour data from SeaWiFS and OCTS will greatly improve our understanding of regions where enhanced biological productivity has implications for commercial fisheries operations. High resolution ocean colour imagery will also play an increasingly valuable role in monitoring variations in seabed topography, habitat type (in appropriately shallow waters), coastal pollution and natural tracers such as river plumes.

There will be an ongoing need, however, for validation of remotely sensed data using conventional (surface-based) measurements, a typical example being the need for *in situ* measurements from surface vessels, buoys, etc. to validate satellite-derived surface ocean temperatures. This is particularly true in tropical areas of high atmospheric water vapour loading, where the accuracy of remotely-sensed SSTs is often poor and SST imagery may not be a reliable indicator of either absolute temperatures or circulation patterns.

The advent of new satellites and sensors will provide increased opportunities for use of complementary sensors in different regions of the electromagnetic spectrum, for example the study of surface circulation patterns using both thermal infrared imagery (to show thermal fronts), altimeter data to derive current speeds and ocean colour imagery to track the movement of tracers such as sediments or plankton patches. Because of the vast expanse of ocean recently proclaimed as Australia's Exclusive Economic Zone (EEZ), satellite remote sensing provides the only feasible means of monitoring both physical and biological processes in our surface waters on a regular basis. Conventional oceanographic measurements are still necessary, however, for providing the full 3-dimensional description of the oceans, so satellite remote sensing must be recognised as only another tool available to the marine scientist.

**Acknowledgements.** This paper has been partly based on information provided by M Grundlingh (CSIR South Africa) as well as by colleagues too numerous to mention individually. Satellite pictures were processed by A Way and C Bowron (CSIRO Division of Oceanography) from imagery supplied by the Western Australian Satellite Technology and Applications Consortium (WASTAC). Landsat TM images have been kindly supplied by P Hick (CSIRO), A Wyllie and R Shaw (WA Department of Land Administration). K Nardi (Abrolhos Islands Consultative Council) and J Stoddart (Marine Science Associates) gave permission to use reports prepared for the Mid-West Development Commission. C Burton undertook the analysis of SST transects off Shark Bay.

## References

Anon 1993 Distribution of marine habitats at the Houtman Abrolhos Islands. I: the Easter Group. Report. Kinhill Engineers, for the Geraldton Mid-West Development Authority. Western Australia, 39 pp.

Anon 1994 Distribution of marine habitats at the Houtman Abrolhos Islands. II: the Wallabi and Southern Groups. Report. Marine Science Associates for the Mid-West Development Commission. Perth, Western Australia, 11 pp.

Baines P G 1981 Satellite observations of internal waves on the Australian North-West Shelf. *Australian Journal of Marine and Freshwater Research* 32:457-463.

Barton I J 1995 Satellite-derived sea surface temperatures: current status. *Journal of Geophysical Research* 100:8777-8790.

Bierwirth P N, Lee T & Burne R V 1993 Shallow sea-floor reflectance and water depth derived by unmixing multispectral imagery. *Photogrammetric Engineering & Remote Sensing* 59:331-338.

Caputi N, Fletcher W J, Pearce A F & Chubb C F 1995 Effect of the Leeuwin Current on the recruitment of fish and invertebrates along the Western Australian coast. *Proceedings of the International Larval Fish Conference. Marine and Freshwater Research* 47:147-155.

Carroll W 1982 The WAIT satellite receiving station. In: *Workshop on Applications of Environmental Satellites* (eds F R Honey & W Carroll), Muresk, CSIRO, Paper 2.1.1, 6 pp.

Catalano P, Wyllie A & Eliot I 1991 Development of a coastal planning information system: Guilderton to Dongara, Western Australia. *Proceedings of the Conference on Remote Sensing and Geographical Information Systems for Coastal Catchment Management*. Lismore, New South Wales, 205-222.

Corner R J & Lodwick G D 1992 Spectral bathymetry using Landsat Thematic Mapper data in Cockburn Sound, Western Australia. *Proceedings of the 6<sup>th</sup> Australasian Remote Sensing Conference* Wellington, New Zealand 1:180-190.

Cresswell G R 1980 Satellite-tracked buoys in the eastern Indian Ocean. *Proceedings of the 14<sup>th</sup> International Symposium on Remote Sensing of the Environment*. Costa Rica, 531-541.

Cresswell G R, Boland F M, Peterson J L & Wells G S 1989 Continental shelf currents near the Abrolhos Islands, Western Australia. *Australian Journal of Marine and Freshwater Research* 40:113-128.

Cresswell G R & Golding T J 1980 Observations of a south-flowing current in the southeastern Indian Ocean. *Deep-Sea Research* 27:449-466.

Cresswell G R & Peterson J L 1993 The Leeuwin Current south of Western Australia. *Australian Journal of Marine and Freshwater Research* 44:285-303.

Easton A, Pearce A F & Buchan S J 1992 Modelling the Kirki spill using OSSM. *Proceedings of the Third National Scientific Support Coordinators Workshop*. Fremantle, Western Australia, 93-96.

Fletcher W J, Tregonning R J & Sant G J 1994 Interseasonal variation in the transport of pilchard eggs and larvae off southern Western Australia. *Marine Ecology Progress Series* 111:209-224.

Fu L-L, Christensen E J, Yamarone C A, Lefebvre M, Menard Y, Dorrer M & Escudier P 1994 Topex/Poseidon mission overview. *Journal of Geophysical Research* 99:24369-24381.

Gee L & Forster B C 1984 Landsat data as an aid to hydrographic and bathymetric mapping in shallow seas. *Proceedings of the 3<sup>rd</sup> Australasian Remote sensing Conference*. Gold Coast, Queensland, 161-173.

Gentili J 1972 Thermal anomalies in the eastern Indian Ocean. *Nature* 238:93-95.

Godfrey J S & Ridgway K R 1985 The large-scale environment of the poleward-flowing Leeuwin Current, Western Australia: longshore steric height gradients, wind stresses and geostrophic flow. *Journal of Physical Oceanography* 15:481-495.

Godfrey J S, Vaudrey D J & Hahn S D 1986 Observations of the shelf-edge current south of Australia, winter 1982. *Journal of Physical Oceanography* 16:668-679.

Griffiths R W & Pearce A F 1985a Satellite images of an unstable warm eddy derived from the Leeuwin Current. *Deep-Sea Research* 32:1371-1380.

Griffiths R W & Pearce A F 1985b Instability and eddy pairs on the Leeuwin Current south of Australia. *Deep-Sea Research* 32:1511-1534.

Hearn C J & Pearce A F 1985 NOAA satellite imagery and airborne remote sensing of a small-scale tidal jet. *Australian Journal of Marine & Freshwater Research* 36:643-653.

- Hick P T & Scoones R 1990 Satellite-derived imagery for water penetration and its relevance to fisheries in the Kimberley region of Western Australia. CSIRO Exploration Geoscience Restricted Report 122R, 29 pp.
- Hick P T, Wyllie A & Kirkman H 1994 Marine substrate feature delineation from Thematic Mapper data: the Geographe Bay example. Proceedings of the 7<sup>th</sup> Australasian Remote Sensing Conference. Melbourne, Australia 3:79-84.
- Hutchins J B & Pearce A F 1994 Influence of the Leeuwin Current on recruitment of tropical reef fishes at Rottnest Island, Western Australia. *Bulletin of Marine Science* 54:245-255.
- Jarvis N 1986 Western Australia, an atlas of human endeavour. Western Australian Department of Lands and Surveys, Perth.
- Lavery P S, Pattiaratchi C B, Wyllie A & Hick P T 1993 Water quality monitoring in estuarine waters using the Landsat Thematic Mapper. *Remote Sensing of Environment* 46:268-280.
- Legeckis R & Cresswell G R 1981 Satellite observations of sea-surface temperature fronts off the coast of western and southern Australia. *Deep-Sea Research* 28:297-306.
- Lenanton R C, Joll L, Penn J & Jones K 1991 The influence of the Leeuwin Current on coastal fisheries of Western Australia. *Journal of the Royal Society of Western Australia* 74:101-114.
- Lynch M J, Prata A J & Hunter J R 1986 Sea surface temperature anomalies off the North West Shelf of Western Australia. Proceedings of the 1<sup>st</sup> Australian AVHRR Conference. Perth, Western Australia, 259-268.
- Maxwell J G H & Cresswell G R 1981 Dispersal of tropical marine fauna to the Great Australian Bight by the Leeuwin Current. *Australian Journal of Marine and Freshwater Research* 32:493-500.
- McMillin L M & Crosby D S 1984 Theory and validation of the multiple window sea surface temperature technique. *Journal of Geophysical Research*, 89:3655-3661.
- Mills D A, D'Adamo N, Wyllie A & Pearce A F 1992 The response of stratified shelf waters to the Leeuwin Current and wind forcing: winter observations off Perth, Western Australia. Proceedings of the 6<sup>th</sup> International Conference on the Physics of Estuaries and Coastal Seas, Margaret River, W. Australia; Mixing in Estuaries and Coastal Seas (ed C B Pattiaratchi). American Geophysical Union. Coastal and Estuarine Studies 50:5-28.
- Morgan G J & Wells F E 1991 Zoogeographic provinces of the Humboldt, Benguela and Leeuwin Current systems. *Journal of the Royal Society of Western Australia* 74:59-69.
- Myers D G & Hick P T 1990 An application of satellite-derived sea surface temperature data to the Australian fishing industry in near real-time. *International Journal of Remote Sensing* 11:2103-2112.
- Pattiaratchi C B 1994 Physical oceanographic aspects of the dispersal of coral spawn slicks: a review. In: The bio-physics of marine larval dispersal (eds P W Sammarco & M L Heron). American Geophysical Union. Coastal and Estuarine Studies 45: 89-105.
- Pattiaratchi C B, Lavery P, Wyllie A & Hick P T 1992 Estimates of water quality in coastal waters using multi-date Landsat Thematic Mapper data. *International Journal of Remote Sensing* 15:1571-1584.
- Pattiaratchi C B, Parslow J, Pearce A F & Hick P T 1990 Application of Coastal Zone Colour Scanner (CZCS) imagery for productivity and circulation studies of the Leeuwin Current, Western Australia. Proceedings of the 5<sup>th</sup> Australasian Remote Sensing Conference. Perth Western Australia, 252-255.
- Pearce A F 1989 A catalogue of NOAA-AVHRR satellite imagery received in Perth, Western Australia, 1981-1987. CSIRO Marine Laboratories Report, CSIRO, Perth, 203, 36 pp.
- Pearce A F 1991 Eastern boundary currents of the southern hemisphere. *Journal of the Royal Society of Western Australia* 74:35-45.
- Pearce A F & Griffiths R W 1991 The mesoscale structure of the Leeuwin Current: a comparison of laboratory models and satellite imagery. *Journal of Geophysical Research* 96:16739-16757.
- Pearce A F & Phillips B F 1988 ENSO events, the Leeuwin Current and larval recruitment of the western rock lobster. *Journal du Conseil* 45:13-21.
- Pearce A F & Prata A J 1990 Sea-surface temperature transects across the Leeuwin Current. Proceedings of the 5<sup>th</sup> Australasian Remote Sensing Conference. Perth, Western Australia, 242-251.
- Pearce A F, Prata A J & Manning C R 1989 Comparison of NOAA-AVHRR-2 sea surface temperatures with surface measurements in coastal waters. *International Journal of Remote Sensing* 10:37-52.
- Pearce A F & Walker D I 1991 The Leeuwin Current. *Journal of the Royal Society of Western Australia* 74:140pp.
- Pellegrini J J & Penrose J D 1986 Comparison of ship-based and satellite AVHRR estimates of sea-surface temperature. Proceedings of the 1<sup>st</sup> Australian AVHRR Conference. Perth, 269-279.
- Phillips B F, Pearce A F & Litchfield R T 1991 The Leeuwin Current and larval recruitment to the rock (spiny) lobster fishery off Western Australia. *Journal of the Royal Society of Western Australia* 74:93-100.
- Prata A J & Lynch M J 1985 Monitoring tropical sea-surface temperature structure from NOAA-AVHRR measurements. Proceedings of the 2<sup>nd</sup> Australian Conference on Tropical Meteorology. Perth, 70-72 (Abstract).
- Prata A J, Pearce A F, Wells J B & Carrier J M 1986 Satellite sea-surface temperature measurements of the Leeuwin Current. Proceedings of the 1<sup>st</sup> Australian AVHRR Conference. Perth, 237-247.
- Prata A J & Wells J B 1990 A satellite sensor image of the Leeuwin Current, Western Australia. *International Journal of Remote Sensing* 11:173-180.
- Robinson I S 1985 *Satellite Oceanography: An Introduction for Oceanographers and Remote-Sensing Scientists*. Ellis Horwood, Chichester.
- Rochford D J 1969 The seasonal interchange of high and low salinity surface waters off South-west Australia. Technical Paper 29, 8 pp. CSIRO Division of Fisheries and Oceanography, CSIRO, Sydney.
- Saunders R W & Kriebel K T 1988a An improved method for detecting clear sky and cloudy radiances from AVHRR data. *International Journal of Remote Sensing* 9:123-150.
- Saunders R W & Kriebel K T 1988b Errata. *International Journal of Remote Sensing* 9:1393-1394.
- Smith R C G 1997 Applications of satellite remote sensing for mapping and monitoring land surface processes in Western Australia. *Journal of the Royal Society of Western Australia* 80:15-28.
- Smith R C G & Pearce A F 1997 A bibliography of research into remote sensing of land, sea and atmosphere in Western Australia. *Journal of the Royal Society of Western Australia* 80:29-39.
- Smith R L, Huyer A, Godfrey J S & Church J A 1991 The Leeuwin Current off Western Australia, 1986-1987. *Journal of Physical Oceanography* 21:323-345.
- Stewart R H 1985 *Methods of Satellite Oceanography*. University of California Press, Berkeley.
- Szekielda K-H & Mitchell W F 1972 Oceanographic applications of color-enhanced satellite imageries. *Remote Sensing of Environment* 2:71-76.
- Tapley I J 1990 The perception of submerged strandlines on night-thermal NOAA-AVHRR satellite imagery. Proceedings of the 5<sup>th</sup> Australasian Remote Sensing Conference. Perth, 2:815-821.
- Wyllie A, Buchanan A, D'Adamo N, Mills D A & Pearce A F 1992 The use of Landsat Thematic Mapper and NOAA AVHRR for environmental investigations of the Perth metropolitan coastal waters. Proceedings of the 6<sup>th</sup> Australasian Remote Sensing Conference. Wellington, New Zealand 3:203-208.